

HiSST: 4th International Conference on High-Speed Vehicle Science Technology 22 -26 September 2025, Tours, France



Investigation of Heat flux and Stagnation Pressure Integrated Measurement Probe using Gardon Gauge

J. Kim*, S. So, K. Park, J. Lee¹, J. Na², M. Kim, D. Hyun³, G. Park⁴, C. Duernhofer, S. Loehle⁵

Abstract

The growing demand for hypersonic vehicle development requires accurate ground testing under appropriate thermal and pressure conditions. This study introduces a novel integrated probe capable of simultaneously measuring heat flux and stagnation pressure for arcjet testing. The apparatus incorporates a water-cooled Gardon gauge and dual stagnation pressure ports in a compact design compliant with ESA standards. Three experimental campaigns were conducted in the PWK4 arcjet facility at IRS, Germany, under both low- and high-enthalpy conditions. Key findings include: (1) a 2 mm pressure port is sufficient for stable stagnation pressure measurement; (2) graphite paste on the Gardon gauge significantly influences heat flux readings, with paste depletion increasing measured flux due to reduced emissivity; (3) the exposed constantan surface exhibits a higher catalytic effect than oxidized copper, leading to elevated heat flux values compared with calorimeter references; and (4) both pressure and heat flux profiles exhibit a bell-shaped distribution, with higher values along the central axis. The integrated probe demonstrated durability, repeatability, and sensitivity to surface conditions, providing a reliable tool for pinpoint heat flux measurements in high-enthalpy arcjet testing.

Keywords: Arcjet, Stagnation Pressure, Heat Flux, Integrated Probe, Gardon Gauge

Nomenclature

ESA - European Space Agency

 $\ensuremath{\mathsf{IRS}}$ - Institute of Space Systems at the

University of Stuttgart

Latin r - radius Greek ε – emissivity

 σ – Stefan-Boltzmann constant

 γ – catalytic efficiency

Subscripts eff - effective surf - surface stag - stagnation

1. Introduction

The growing significance of hypersonic vehicle research has necessitated accurate ground testing under extreme thermal and aerodynamic conditions. Arcjet plasma systems serve as critical facilities for evaluating hypersonic propulsion systems, atmospheric re-entry vehicles, and related technologies, as they are capable of generating extremely high-temperature flows on the order of several thousand

HiSST-2025-0005 Page | 1 Investigation of Heat flux and Stagnation Pressure Integrated Measurement Probe using Gardon Gauge

¹ ADD (Agency for Defense Development), Daejeon, Korea. *: kjw8211@gmail.com

² SNU (Seoul National University), Seoul, Korea

³ Vitzro nextech, Ansan, Korea

⁴ KAIST (Korea Advanced Institute of Science and Technology), Daejeon, Korea

⁵ IRS (Institut für RaumfahrtSysteme), Stuttgart, Germany

degrees Kelvin. Numerous studies have been conducted to quantify key parameters of arcjet plasma systems, including heat flux, stagnation pressure, specific enthalpy, and surface temperature. For instance, Auweter-Kurt et al. introduced various measurement techniques implemented in the plasma wind tunnels at IRS, Germany, highlighting the importance of these parameters [1].

Among these, heat flux measurement has been widely studied and can be broadly classified into two categories: steady and unsteady methods. Steady measurement systems, such as calorimeters and Gardon gauges, employ water-cooling mechanisms that enable operation in the harsh arcjet plasma environment for durations exceeding several tens of seconds. In contrast, unsteady systems—such as slug calorimeters and null-point sensors—lack cooling mechanisms, which limits their operational duration but offers advantages of structural simplicity and ease of implementation [2–4].

To comprehensively characterize arcjet flow fields, it is advantageous to employ integrated probes capable of simultaneously measuring heat flux and stagnation pressure within a single test. One approach reported in literature involves positioning the heat flux and stagnation pressure measurement systems on opposite sides of the probe, then rotating the probe by 180° to acquire both measurements sequentially [5]. Hermann et al. also used a probe for measure heat flux and stagnation pressure together in a single test [6].

This study presents a newly developed apparatus—hereafter referred to as the integrated probe—designed to simultaneously measure heat flux and stagnation pressure under arcjet flow conditions. To incorporate the heat flux sensing capability, a Gardon gauge was selected due to its robustness and proven accuracy in high-temperature environments [7]. The Gardon gauge consists of a thin constantan foil mounted on a copper cylinder. Incident heat flux raises the central temperature of the foil, creating a radial temperature distribution. While the relationship between temperature and heat flux is nonlinear, the thermoelectric characteristics of constantan and copper produce a linear relationship between the generated electromotive force (EMF) and the incident heat flux. Thus, by measuring the EMF, the heat flux can be determined. The concept and a photograph of the Gardon gauge are shown in Fig. 1.

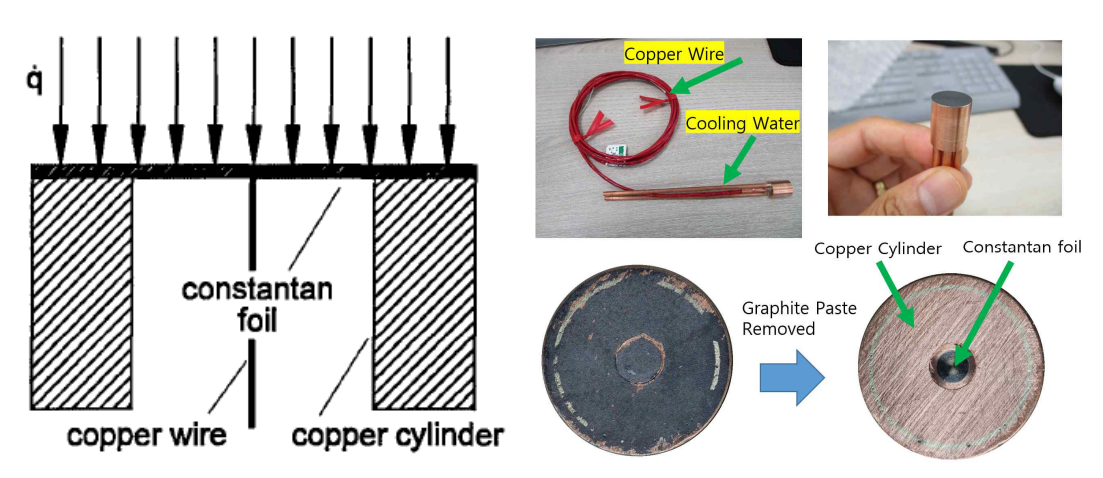


Fig 1. Concept and photograph of Gardon gauge

2. Experimental Overview

Based on the identified need for simultaneous acquisition of heat flux and stagnation pressure data in arcjet environments, an integrated probe was conceived and developed to address the limitations of conventional sequential measurement techniques. The design process prioritized robustness under extreme thermal loads, and compatibility with existing arcjet facility interfaces. This section provides an overview of the integrated probe configuration, the experimental facility, and the operational conditions under which the tests were conducted.

2.1. Integrated Probe

A water-cooled Gardon gauge was selected for heat flux measurement. The copper cylinder of the Gardon gauge has an outer diameter of 12.7 mm, and the constantan foil has a diameter of

approximately 3 mm. In its unused condition, the constantan foil is coated with graphite paste to improve surface emissivity. The voltage signal is obtained through copper leads connected directly to the constantan foil, and the heat flux is calculated from this voltage using a pre-determined calibration sheet.

Fig. 2 shows the schematic of the integrated probe designed for simultaneous measurement of heat flux and stagnation pressure. The Gardon gauge is mounted inside a 50 mm-diameter probe body with an 11.5 mm-radius corner, in accordance with ESA standards [8]. Insulation between the Gardon gauge and the probe body is provided by a ceramic ring. Two stagnation pressure holes, each with a diameter of 2 mm, are located on the frontal surface of the probe, symmetrically positioned on the left and right side of the Gardon gauge. The pressure measurement lines, cooling water tubes for the Gardon gauge, and copper signal leads pass through 20 mm-diameter openings at the bottom of the probe and are connected to the facility interfaces. The probe body itself is also equipped with an independent water-cooling system.

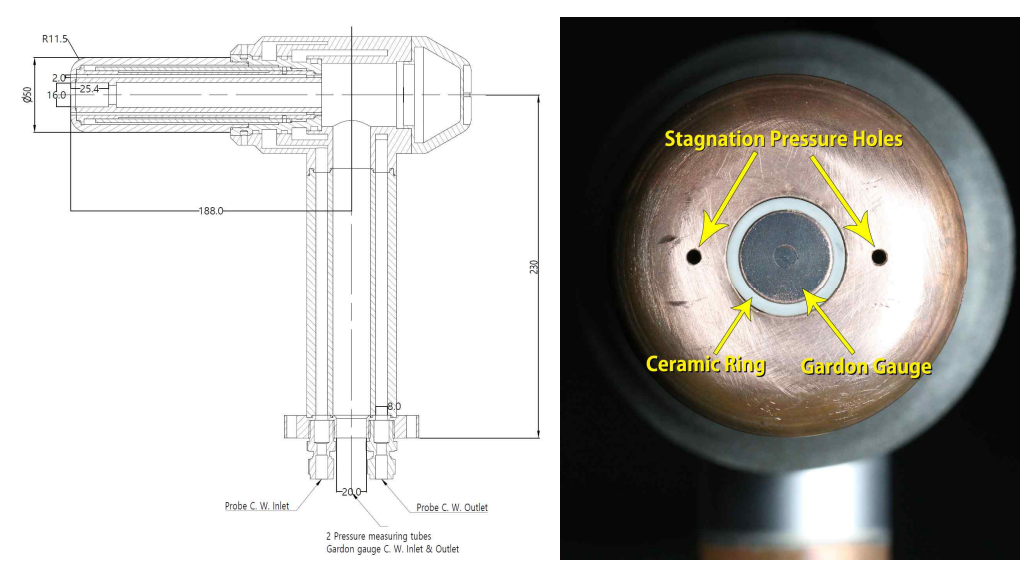


Fig 2. Schematic and annotated photograph of the integrated probe

2.2. Test Facility and Conditions

The experiments were conducted in the PWK4 arcjet plasma facility at the Institute of Space Systems (IRS), Germany [9]. Fig. 3 presents an overview of the facility along with the integrated probe installed in the test section.





Fig 3. PWK4 facility and installed integrated probe

Fig. 4 illustrates the experimental setup in PWK4. The signal from the Gardon gauge was amplified using an in-house–developed amplifier with a gain factor of 200. The amplifier incorporated a low-pass RC filter (R = 10 k Ω , C = 2 nF) yielding a cut-off frequency of fo = 7.96 kHz, as well as an AD210 isolation amplifier. The two stagnation pressure lines were routed to pressure transducers located

HiSST-2025-0005 Page | 3

outside the test cell: one connected to an MKS 0–100 mbar type 622AX12MDE, and the other to an MKS 0–100 mbar type 622D12TDE. All signals were logged using a Datascan 7320 data acquisition unit. In addition, the Gardon gauge signal was simultaneously recorded using a Teledyne LeCroy Wavesurfer 24XS-A oscilloscope to achieve a higher temporal resolution.

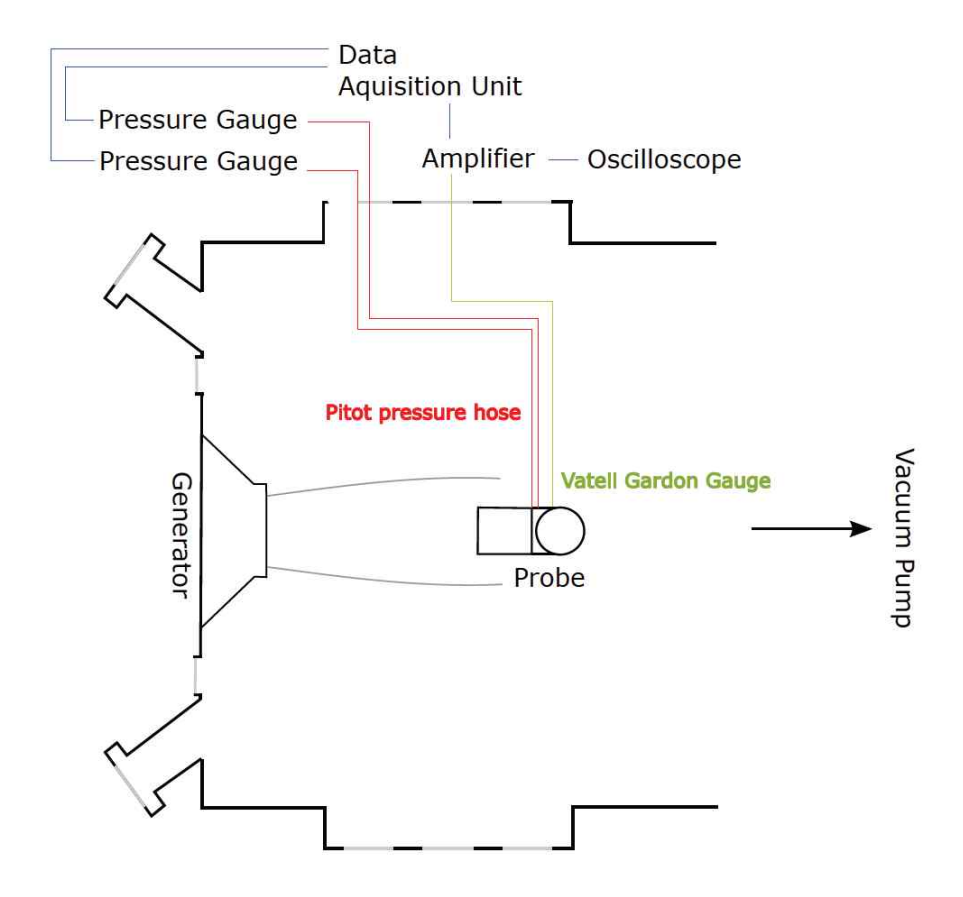


Fig 4. Experimental setup schematic for the PWK4 facility

The PWK4 facility is a well-established arcjet test platform where numerous experimental campaigns have been conducted. Comparative tests between NASA Ames and PWK4 have been previously performed, and in this study, the test conditions were selected to match those of the NASA–IRS collaborative experiments [10]. The selected test conditions are summarized in Table 1.

Table 1. Test Conditions

	Low condition	High Condition
Air mass flow \dot{m}_{air}	6.52 g/s	5 g/s
Arc current I	530 A	740 A
Arc voltage U	88.5 V	83 V
${\sf x}$ - position x	80 mm	76 mm
Magnetic current I_{mag}	120 A	120 A
Ambient pressure p_{amb}	0.4 hPa	6.6 hPa
Reference heat flux \dot{q}	$791 \mathrm{kW/m^2}$	$2412\mathrm{kW/m^2}$
Reference pitot pressure p_{tot}	12.4 hPa	40 hPa

Prior to installing the integrated probe, reference tests were conducted using the IRS "Double probe" (Fig. 5) [5]. One side of the probe is equipped with a calorimeter that determines heat flux based on the cooling water flow rate and the temperature difference between inlet and outlet. The opposite side

contains a stagnation pressure port. The probe head has a diameter of 50 mm and a corner radius of 11.5 mm, consistent with the ESA standard and identical to the integrated probe design.

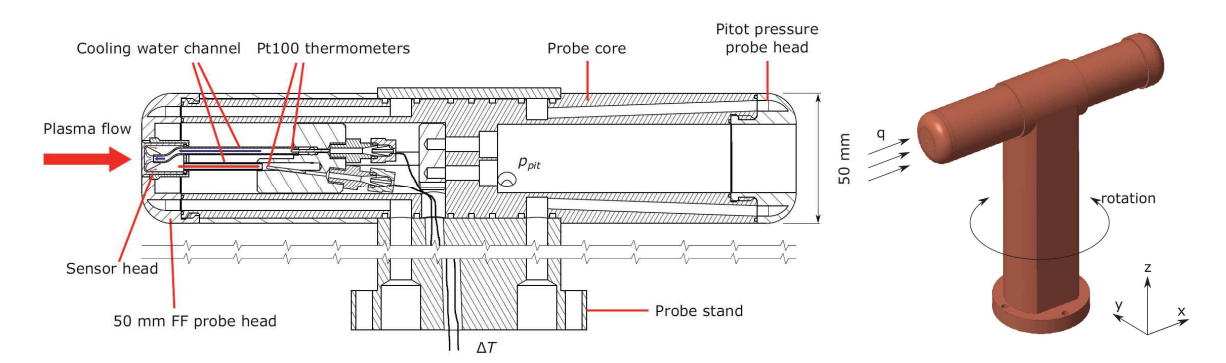


Fig 5. Schematic of the IRS double probe

Once the reference heat flux and stagnation pressure conditions were established, the integrated probe was installed and the same low- and high-condition tests were repeated. Three experimental campaigns were carried out, comprising a total of 67 runs, as summarized below:

- Campaign #1: Exp1 7 Runs, Exp2 8 Runs, Exp3 2 Runs
- Campaign #2: Exp1 6 Runs, Exp2 6 Runs, Exp3 6 Runs
- Campaign #3: Exp1 4 Runs, Exp2 6 Runs, Exp3 10 Runs, Exp4 6 Runs, Exp5 6 Runs

HiSST-2025-0005 Page | 5 Investigation of Heat flux and Stagnation Pressure Integrated Measurement Probe using Gardon Gauge

3. Results and Discussion

3.1. Campaign #1

40

35

[hPaA]

Pressure 02

In Campaign #1, the stagnation pressure measurements failed to establish a steady-state region for all test sequences (Exp1–Exp3), as shown in Fig. 6. This slow pressure build-up is attributed to the excessive length of the pressure tubing. In the current configuration, the existing probe is connected to the facility through several meters of 1/16-inch tubing, followed by additional sections of larger-diameter tubing. To improve the response time and establish a steady-state region, the pressure transducers should be positioned as close to the probe as possible in Campaign #2.

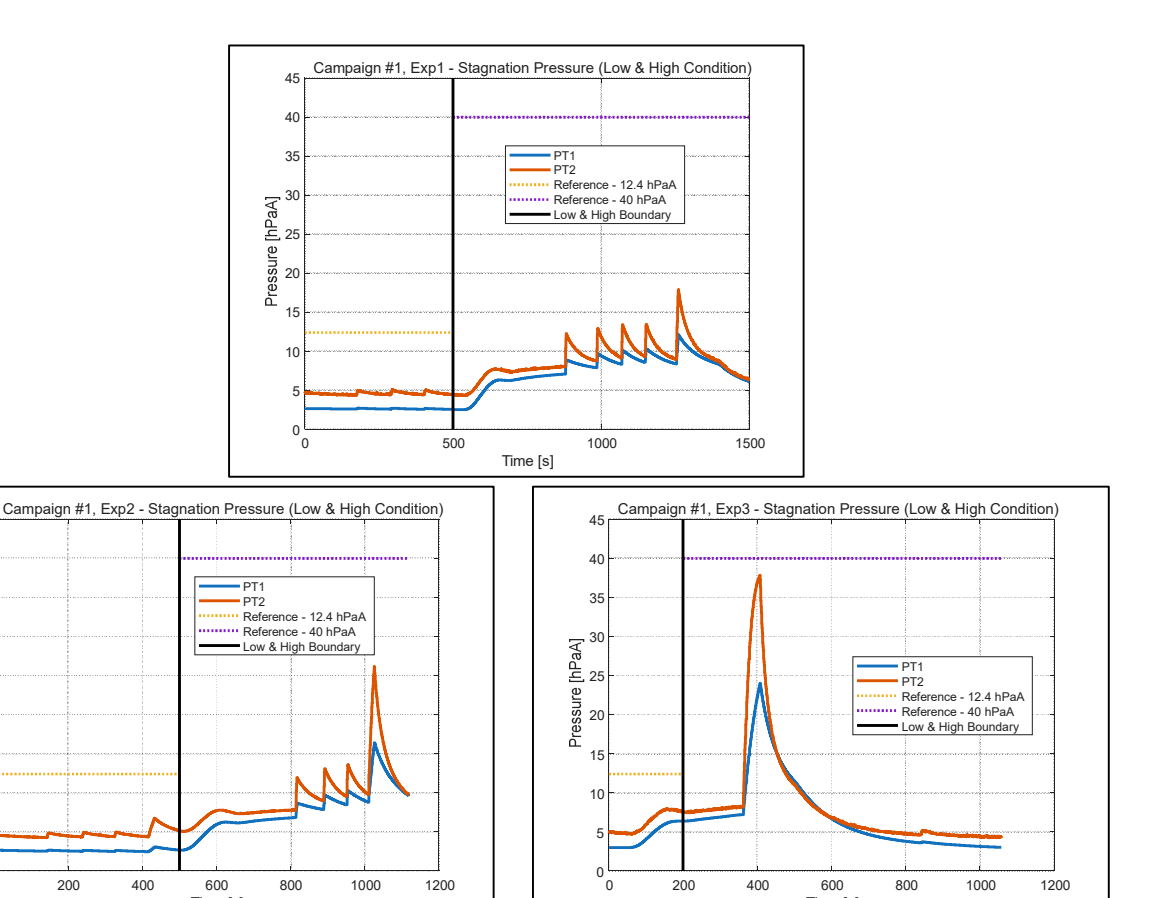
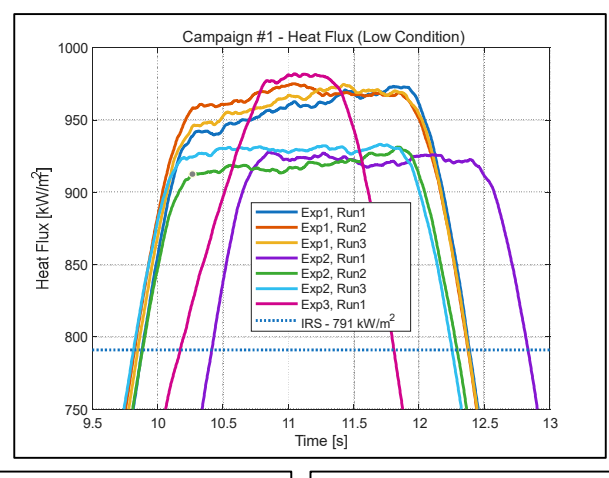
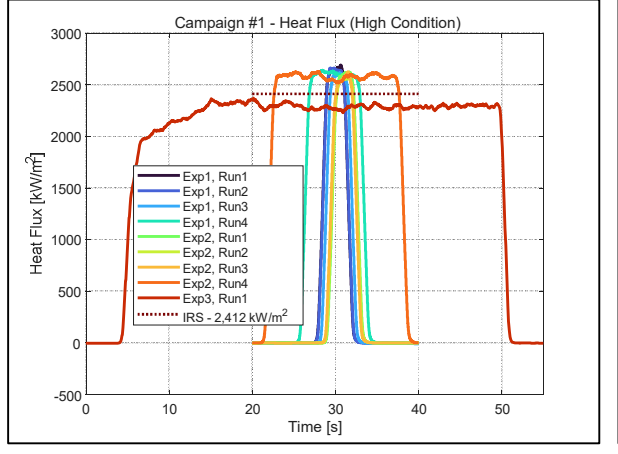


Fig 6. Stagnation pressure measurements from Campaign #1

The heat flux results are presented in Fig. 7. The testing sequence was conducted in the following order: $Exp1-Low \rightarrow Exp1-High \rightarrow Exp2-Low \rightarrow Exp2-High \rightarrow Exp3-Low \rightarrow Exp3-High.$ The upper part depicts the results under low condition, the bottom-left part corresponds to the high condition, and the bottom-right part presents a magnified view of the high condition data. Across all runs, consistent trends were observed. With the exception of the Exp3 high-condition test, measured heat flux values exceeded the IRS reference values (dotted lines). In Exp3, the heat flux remained constant for the full 45-second duration, indicating stable operation under high thermal loads.





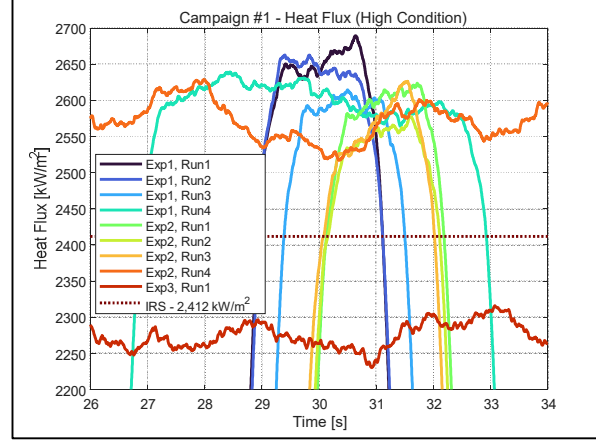


Fig 7. Heat flux measurements from Campaign #1

The summarized results for Campaign #1 are provided in Table 2. Overall, although the stagnation pressure measurements were limited by tubing-induced response delays, the integrated probe demonstrated repeatability and reliability, as consistent heat flux readings were obtained in successive runs. Furthermore, the 45-second stable measurements in Exp3 confirm the probe's thermal durability.

The Gardon gauge employed in Campaign #1 had an upper heat flux limit of 30,000 kW/m², substantially higher than the maximum measured value of 2,412 kW/m² under high-condition tests. For improved resolution, a more sensitive Gardon gauge will be prepared for Campaign #2. Additionally, the pressure measurement system will be modified to minimize tubing length and improve dynamic response.

HiSST-2025-0005 Page | 7 Investigation of Heat flux and Stagnation Pressure Integrated Measurement Probe using Gardon Gauge

Exp. Name	Exp. Conditions	Run #	Results
Exp1		Run 1	968
	Low - 791 kW/m^2	Run 2	967
		Run 3	971
		Run 1	2,669
	High – 2,412 kW/m^2	Run 2	2,651
		Run 3	2,614
		Run 4	2,611
Exp2		Run 1	925
	Low – 791 kW/m^2	Run 2	926
		Run 3	931
		Run 4	939
		Run 1	2,611
	High – 2,412 kW/m^2	Run 2	2,571
		Run 3	2,624
		Run 4	2,584
F2	Low - 791 kW/m^2	Run 1	981
Exp3	High - 2,412 kW/m^2	Run 1	2,292

Table 2. Campaign #1 results

3.2. Campaign #2

Following the results of Campaign #1, maximum limit 5,000 kW/m^2 Gardon gauge was prepared, and the pressure gauge was installed inside the test cell to minimize the pressure tubing length. Fig. 8 presents the stagnation pressure results. The stagnation pressure data exhibited a stable, flat profile in all cases, confirming that minimizing the pressure tubing length was effective and that a 2 mm diameter tube was sufficient for accurate measurement. However, all measured values were slightly lower than the IRS reference values.

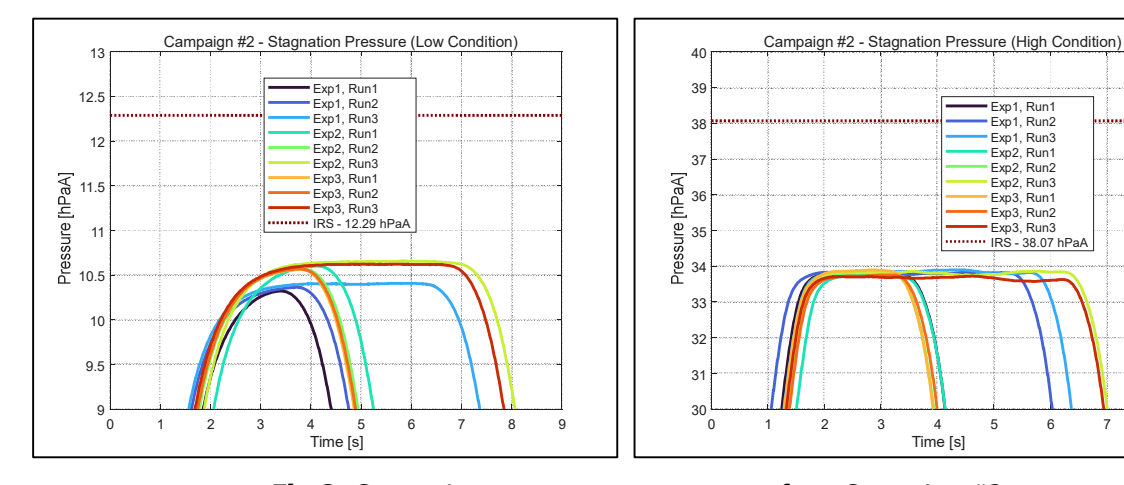


Fig 8. Stagnation pressure measurements from Campaign #2

Fig. 9 presents heat flux results. the three columns correspond to Exp1, Exp2, and Exp3. The upper rows indicate low-condition test results, while the lower rows represent high-condition tests. The test sequence was Exp1 Low \rightarrow Exp1 High \rightarrow Exp2 Low \rightarrow Exp2 High \rightarrow Exp3 Low \rightarrow Exp3 High. All measured heat flux values were higher than the IRS reference. In Exp1 and Exp2, the same Gardon gauge (#11177) was used, while Exp3 employed another gauge of identical maximum limit (#11176). A notable trend was observed in the brand-new Gardon gauge: heat flux readings tended to increase with each run under low-condition tests (Exp1 & Exp3). In Exp2, the heat flux remained stable for both low and high conditions, consistently exceeding the reference values, though with smaller deviations compared to Exp1.

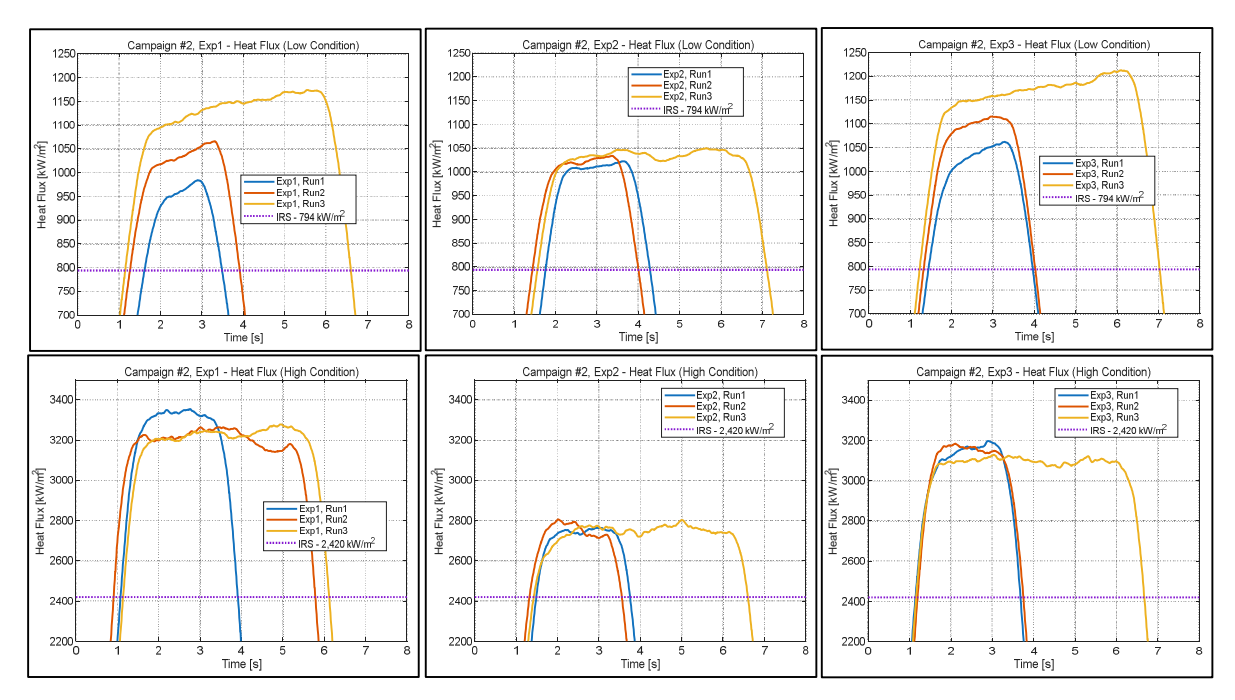


Fig 9. Heat flux measurements from Campaign #2

Table 3 summarizes the Campaign #2 results. The deviation rate was calculated using Eq. (1):

Deviation Rate
$$[\%] = \frac{\text{M easured Value - Reference Value}}{\text{Reference Value}} \times 100$$
 (1)

The deviation rate for stagnation pressure ranged from approximately -16% to -11%. For the brand-new Gardon gauge, the deviation increased from approximately 20% to 50% (highlighted in the green box). Exp2 under high conditions exhibited the smallest deviation, around 14%, compared to Exp1 and Exp3 high-condition tests (highlighted in the red box).

	Exp. Conditions	Run # Gardon gauge	Caudan	Heat Flux		Stag. Pressure	
Name			Measure [kW/m^2]	Deviation Rate	Measure [hPaA]	Deviation Rate	
	Low (794 kW/m², 12.29 hPaA)	1 (2s)	#11177 (Max 5,000 kW/m^2)	983	23.8%	10.3	-16.2%
		2 (2s)		1,066	34.3%	10.4	-15.4%
Exp1		3 (5s)		1,171	47.5%	10.4	-15.4%
Exbī	High (2,420 kW/m², 38.07 hPaA)	1 (2s)		3,350	38.4%	33.8	-11.2%
		2 (2s)		3,264	34.9%	33.8	-11.2%
		3 (5s)		3,276	35.4%	33.8	-11.2%
	Low (794 kW/m², 12.29 hPaA)	1 (2s)		1,022	28.7%	10.6	-13.8%
		2 (2s)		1,039	30.9%	10.6	-13.8%
F1/102		3 (5s)		1,050	32.2%	10.6	-13.8%
Exp2	High (2,420 kW/m², 38.07 hPaA)	1 (2s)		2,764	14.2%	33.8	-11.2%
		2 (2s)		2,761	14.1%	33.8	-11.2%
		3 (5s)		2,770	14.5%	33.8	-11.2%
Exp3	Low (794 kW/m², 12.29 hPaA)	1 (2s)	#11176 (Max 5,000 kW/m^2)	1,062	33.8%	10.6	-13.8%
		2 (2s)		1,116	40.6%	10.6	-13.8%
		3 (5s)		1,212	52.6%	10.6	-13.8%
	High (2,420 kW/m², 38.07 hPaA)	1 (2s)		3,196	32.1%	33.7	-11.5%
		2 (2s)		3,166	30.8%	33.7	-11.5%
		3 (5s)		3,124	29.1%	33.7	-11.5%

Table 3. Campaign #2 Results

A clear correlation was found between the number of runs and heat flux increase during low-condition tests when using a newly installed gauge. As illustrated in Fig. 10, the graphite paste coating on the

HiSST-2025-0005 Page | 9
Investigation of Heat flux and Stagnation Pressure Integrated Measurement Probe using Gardon Gauge
Copyright © 2025 by author(s)

Gardon gauge gradually wore off after successive runs, and under high conditions (Fig. 11), no residue remained after testing.



Fig 10. Condition of graphite paste during Exp3 Runs 1-3 (Low Condition)



Fig 11. Condition of graphite paste during Exp3 Runs 1–3 (High Condition)

When heat flux impinges on the probe surface, the surface energy balance is expressed as Eq. (2) [11]:

$$\dot{q}_{surf} = Re - Radiation + Conduction + Abbation$$

$$= 80 T_{surf}^4 + Conduction + Abbation \qquad (2)$$

Because the constantan foil in the Gardon gauge is extremely thin (~0.07 mm), conduction losses are negligible, and no ablation occurs due to water cooling. Consequently, the only significant term in the energy balance is re-radiation. The heat flux arriving at the gauge's surface (\dot{q}_{surf}) is constant during Run 1~3. However, as the graphite paste (ε =0.82) wears off the bare constantan surface (ε =0.44) is exposed, reducing emissivity, increasing surface temperature, and thereby increasing the measured heat flux. This explains the observed increasing trend in heat flux during the low condition tests of Exp1 and Exp3.

The lower heat flux values in Exp2 compared to Exp1 are attributed to changes in the constantan surface. Several hours after Exp1, oxidation of the bare constantan likely reduced its catalytic activity. The catalytic effect—the recombination of gas-phase species on the surface—should be considered when $r_{eff} \times p_{stag} < 1.0 \ [am * atm] \ [12]$. In order to calculate r_{eff} , we should define r_B : Body Radius, r_N : Now Radius, r_C : Corner Radius [13]. Following ESA Standard geometry, $r_B = 25 \, m \, m$, $r_C =$ 11.5 mm Because the probe is flat faced, $r_N = \infty$. Based on Ref. [13], r_{eff} is calculated as 62.5 mm. The stagnation pressures for the low and high conditions are 12.4 hPaA and 40 hPaA, respectively, resulting in $r_{eff} \times p_{stag} = 0.08$ and 0.23 [cm * atm]. These values confirm that catalytic effects must be considered for both test conditions.

As catalytic activity increases, more particles recombine at the stagnation point, releasing recombination energy and increasing the measured heat flux. Fig. 12 illustrates the contribution of this recombination energy to the overall heat flux, as induced by the catalytic effect [14].

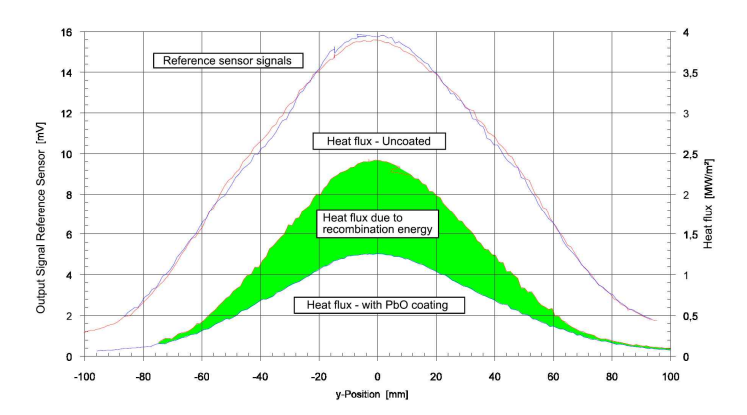


Fig 12. Effect of catalytically induced heat flux [14]

The catalytic effect provides a clear explanation for why the heat flux measured by the Gardon gauge is consistently higher than that of the IRS reference calorimeter. This effect is directly related to the catalytic efficiency (γ) of the surface material; the higher the γ , the stronger the catalytic effect and the greater the resulting heat flux. The IRS calorimeter is made of copper (Cu), which is initially fully catalytic, with a catalytic efficiency above 0.1. However, after only a few seconds in arcjet flow, pure copper oxidizes to copper oxide (CuO), reducing its catalytic efficiency to approximately 0.02 [15]. In contrast, the constantan material of the Gardon gauge has a catalytic efficiency above 0.046 [16]. Since this value is higher than that of CuO, the constantan surface induces greater recombination energy at the stagnation point, resulting in higher heat flux measurements. Over time, oxidation of constantan also reduces its catalytic efficiency. This explains why, in Campaign #2, Exp2 recorded lower heat flux values than Exp1, even under similar conditions.

3.3. Campaign #3

Insights from Campaigns #1 and #2 guided the planning of Campaign #3, which served as the final testing opportunity. Several unresolved issues were addressed through five targeted experiments:

- Exp1 Investigate stagnation pressure differences between the central axis and an off-axis
- Exp2 Reverse the test sequence from the usual low \rightarrow high condition to high \rightarrow low condition.
- Exp3 Remove all graphite paste to assess its effect, and compare heat flux at central and off-axis positions.
- Exp4 Apply a thicker graphite paste layer to examine its influence.
- Exp5 Continuation of Exp4.

3.3.1. Exp1- Central vs. Off-Axis Stagnation Pressure

In the previous campaigns, stagnation pressure readings were consistently lower than the IRS reference. In Exp1, the Gardon gauge at the central axis was replaced with a dedicated stagnation pressure measurement port (Fig. 13).

HiSST-2025-0005 Page | 11 Investigation of Heat flux and Stagnation Pressure Integrated Measurement Probe using Gardon Gauge

Fig 13. Central axis stagnation pressure measurement setup

The left (L) pressure line previously used for off-axis measurement was reconfigured to measure the central axis (C) pressure. This allowed for simultaneous measurements at the right (R) and central (C) positions. Two runs were performed under both low and high conditions. The results showed that, as in Campaigns #1 and #2, the (R) stagnation pressure remained lower than the IRS reference, whereas the central axis (C) pressure was higher (Fig. 14). This aligns with the known pressure profile in arcjet flow, where stagnation pressure decreases from the center toward the periphery.

And RS stagnation pressure measurement represents an average value over a 25 mm diameter flow region. This averaged pressure lies between the stagnation pressures measured at the right (R) and Central (C) positions. In contrast, the integrated probe provides a localized stagnation pressure measurement within a 2 mm diameter area, capturing pin-point flow conditions.

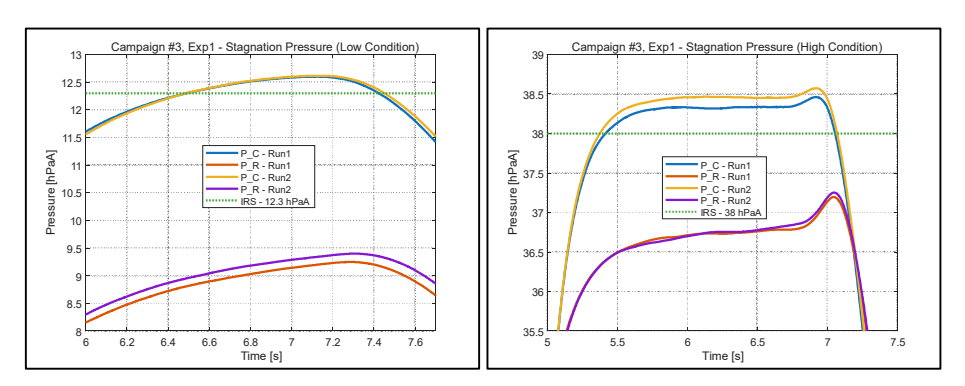
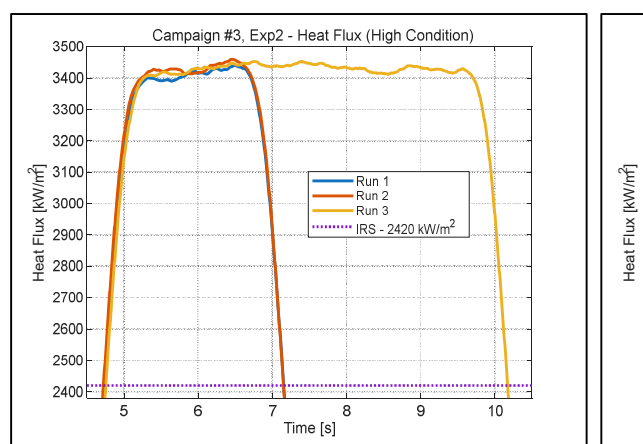


Fig 14. Comparison of stagnation pressure at central and right positions

3.3.2. Exp2 - High-to-Low Test Sequence

Campaign #2 revealed that a brand-new Gardon gauge exhibited a gradual increase in heat flux readings over successive runs, attributed to graphite paste wear. In Exp2, the sequence was reversed to high \rightarrow low to verify whether the trend persisted. Unfortunately, during the initial high condition run (Run 0), heat flux data was lost due to an oscilloscope maximum limit error. The following runs (Run 1-3) proceeded as planned. Heat flux values remained consistent across all high- and low-condition runs, with no observable gradual increase. It is presumed that the initial high-condition Run 0 had already removed much of the graphite paste, eliminating the wear effect (Fig. 15).

HiSST-2025-0005 Page | 12 J. Kim, S. So, K. Park, J. Lee, J. Na, M. Kim, D. Hyun, G. Park, C. Duernhofer, S. Loehle



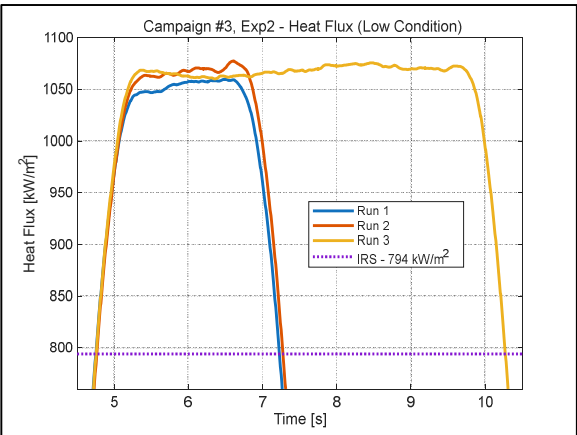


Fig 15. Heat flux results for High-to-Low test sequence

3.3.3. Exp3 - Effect of Graphite Paste Removal and Off-Axis Measurements

Exp3 was conducted with all graphite paste removed from the Gardon gauge to assess its influence. The experiment also compared heat flux between central and off-axis positions.

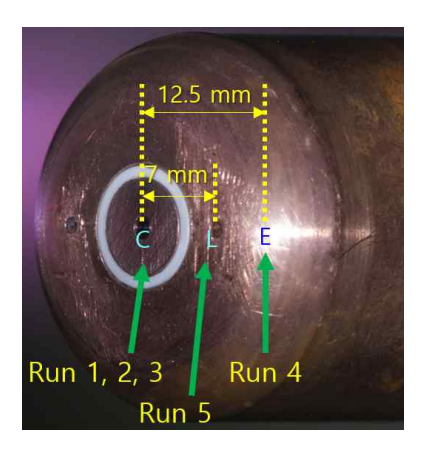


Fig 16. Heat flux measurement positions

Runs 1-3 measured heat flux at the center axis. Run 4 was offset by 12.5 mm to match the IRS stagnation pressure measurement area. Run 5 was offset by 7 mm to align with the IRS heat flux measurement area (Fig. 16). Results showed a clear decrease in heat flux with increasing distance from the center. Across all positions, however, values remained higher than the IRS reference, reaffirming that the catalytic effect of bare constantan exceeds that of CuO (Fig. 17). The IRS heat flux value represents the average over a 14 mm diameter circle (Fig. 5), while the Gardon gauge measures a pinpoint value (~3 mm diameter). Because the arcjet flow profile is bell-shaped with peak intensity at the center, pinpoint readings at the center exceed the IRS average (Fig. 18). Similar positional effects were also observed for stagnation pressure.

HiSST-2025-0005 Page | 13 Investigation of Heat flux and Stagnation Pressure Integrated Measurement Probe using Gardon Gauge

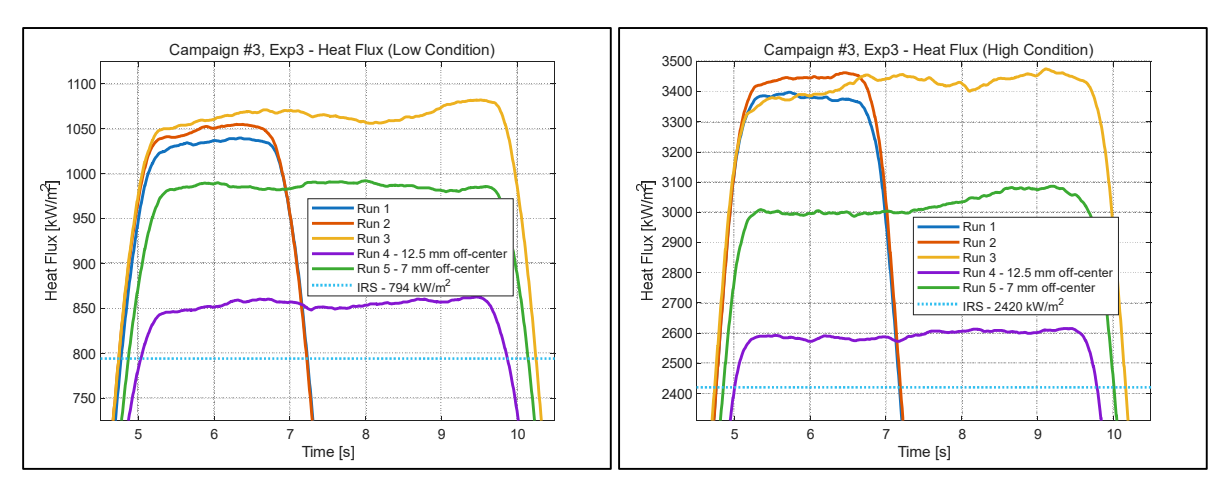


Fig 17. Heat flux measured at different radial positions

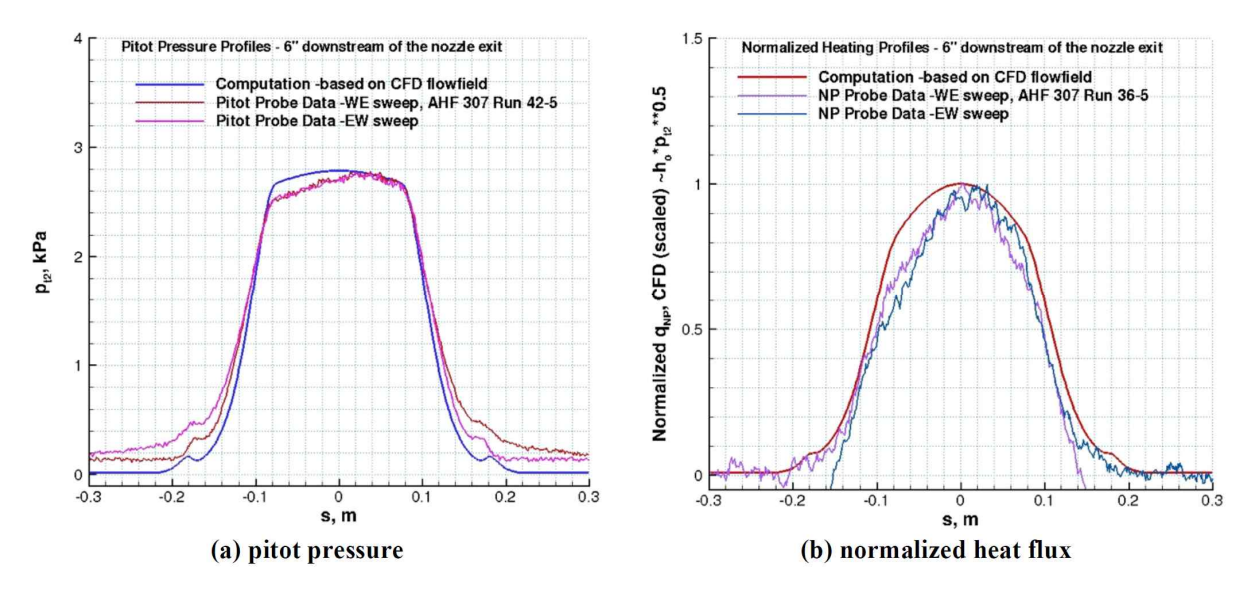


Fig 18. Arcjet flow profile [17]

3.3.4. Exp4 & Exp5 - Effect of Thick Graphite Paste

In Exp4, a thicker layer of graphite paste was applied to the Gardon gauge to investigate its influence on heat flux measurements. Under the Low Condition, three consecutive runs were performed. The measured heat flux remained at approximately 310 kW/m², significantly lower than the IRS reference value of 794 kW/m². This reduction is attributed to the thick graphite layer acting as a thermal barrier, preventing heat from reaching the Gardon gauge. In the High Condition, as the runs progressed (Run $1 \rightarrow \text{Run } 3$), the graphite paste gradually peeled off, causing a marked increase in heat flux. Notably, during Run 1, a sudden rise in heat flux was observed at the moment the paste detached, after which the heat flux stabilized in Runs 2 and 3 at around 4,400 kW/m²—the highest value recorded in all campaigns. This phenomenon, which is due to the concentration of heat in the craters, parallels localized heat concentration damage seen in historical aerospace incidents, such as the Space Shuttle Columbia accident.

In Exp5, testing was conducted immediately after the craters formed in Exp4. Under the Low Condition, Run 1 began with a high heat flux of 1,620 kW/m² due to the crater effect, but as Runs 1–3 progressed, the craters gradually flattened, reducing the heat flux to 1,600 kW/m². Under the High Condition, crater flattening continued, producing a steady decline in heat flux from 4,300 kW/m² in Run 1 to 3,900 kW/m² in Run 3. These results underscore that the presence, thickness, and degradation pattern of

graphite paste critically affect measured heat flux, with crater formation significantly amplifying localized heating.

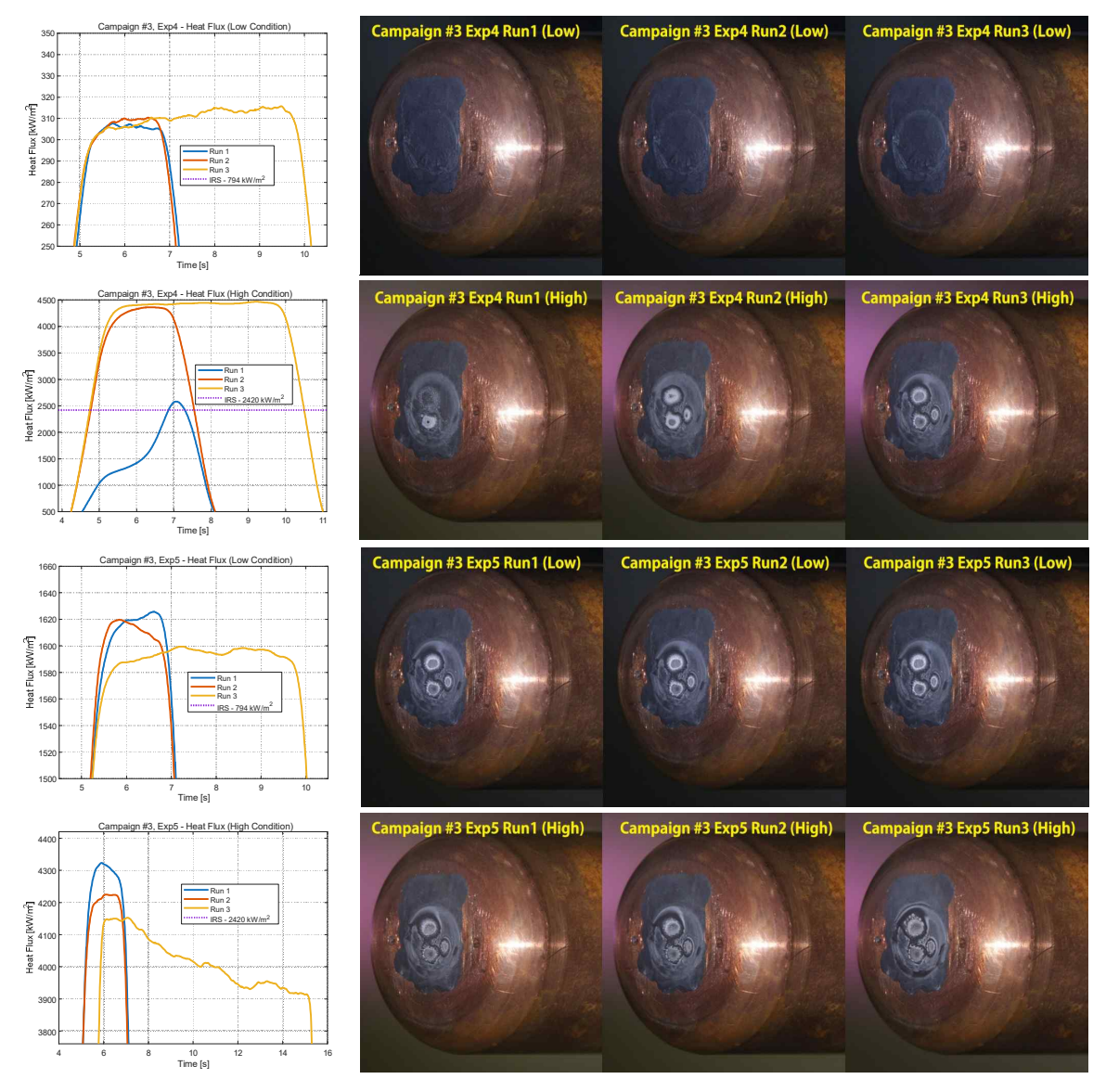


Fig 19. Heat flux variation during graphite paste wear

Name	Exp. Conditions	Run #	Time [s]	Heat Flux [kW/m^2]	Stagnation Pressure [hPaA]	Remarks	
Exp1	Low – 794 kW/m^2, 12.3 hPaA	Run 1, 2	2, 2	Not Used	Center(C) 12.6 Right(R) 9.4	Center(C) Pressure is bigger than 12.5 mm off-center Right(R) Pressure	
	High – 2,420 kW/m^2, 38.0 hPaA	Run 1, 2	2, 2	Not used	Center(C) 38.5 Right(R) 36.9		
E.m.a	High – 2,420 kW/m^2, 38.0 hPaA	Run 1, 2, 3	2, 2, 5	3,442, 3,460, 3,453	10.8, 11.0, 11.2	Heat flux remained	
Exp2	Low – 794 kW/m^2, 12.3 hPaA	Run 1, 2, 3	2, 2, 5	1,060, 1,077, 1,076	37.1, 37.1, 37.1	constant.	
Exp3	Low – 794 kW/m^2, 12.3 hPaA	Run 1, 2, 3, 4, 5	2, 2, 5, 5, 5	1,040, 1,055, 1,082, 863, 992	Run1~3: Center Heat Flux Run4: 12.5 mm off-center Heat Flux Run5: 7 mm off-center Heat Flux Heat flux decreases as one moves away from the central axis.		
	High – 2,420 kW/m^2, 38.0 hPaA	Run 1, 2, 3, 4, 5	2, 2, 5, 5, 5	3,398, 3,463, 3,475, 2,615, 3,087			
	Low – 794 kW/m^2, 12.3 hPaA	12.3 hPaA 3 2, 2, 5 - Heat Flux was measured lower as 310 kW/					
Exp4	High – 2,420 kW/m^2, 38.0 hPaA	Run 1, 2, 3	2, 2, 5	Condition. - Heat Flux was measured higher as 4,400 kW/m^2 in High Condition due to the concentration of heat in craters.			
	Low – 794 kW/m^2, 12.3 hPaA	Run 1, 2, 3	2, 2, 5	 Low: the heat flux was initially measured high at 1,620 kW/m^2 due to the crater effect, but as Runs 1 ~ 3 progressed, the craters flattened out, reducing the heat flux to 1,600 kW/m^2. High: The craters flattened further, resulting in a continuous decrease in heat flux from 4,300 kW/m^2 to 3,900 kW/m^2. 			
Exp5	High – 2,420 kW/m^2, 38.0 hPaA	Run 1, 2, 3	2, 2, 10				

Table 4. Campaign #3 results

4. Conclusion

An integrated probe capable of simultaneously measuring heat flux and stagnation pressure was designed, fabricated, and validated through a series of arcjet experiments. The main findings are as follows:

- Stagnation Pressure Measurement A 2 mm diameter orifice is sufficient for accurate stagnation pressure measurements.
- Graphite Paste as a Measurement Variable The thickness and condition of the graphite paste applied to the Gardon gauge significantly influence measured heat flux values.
- Graphite Paste Depletion Effect In arcjet flows, depletion of graphite paste decreases surface emissivity, which increases the measured heat flux. For high-enthalpy environments, preremoval of the paste can yield more stable readings.
- Catalytic Surface Effect When graphite paste is absent, the high catalytic efficiency of Constantan produces higher heat flux readings than CuO-coated copper surfaces. As Constantan oxidizes over time, catalytic efficiency decreases, reducing measured heat flux.
- Flow Profile Observations The arcjet flow exhibits a bell-shaped heat flux and stagnation pressure profile, with peak values at the centerline decreasing toward the periphery. Pin-point measurements from the integrated probe are inherently higher than the area-averaged values from calorimeters.
- Calibration Potential Post-test calibration after graphite paste removal can help reconcile systematic offsets between Constantan-based Gardon gauges and calorimeter measurements, enabling accurate pin-point heat flux assessment.
- Localized Heating in Crater Formations Concentration of heat flux into crater-shaped defects on the graphite layer can cause extreme localized heating, a phenomenon relevant to thermal protection system failure analysis.

Acknowledgement

This work was supported by the ADD (Agency for Defense Development) Grant Funded by the Korean Government (UG243006UD).

References

- 1. Auweter-Kurtz, M., Feigl, M., Winter, M.: Diagnostic Tools for Plasma Wind Tunnels and Reentry Vehicles at the IRS. RTO AVT Course on "Measurement Techniques for High Enghalpy and Plasma Flows", held in Rhode-Saint-Genese, Belgium, (2000)
- 2. Terrazas-Salinas, I., Carballo, J.E., Driver, D.M.: Comparison of Heat Transfer Measurement Devices in Arc Jet Flows with Shear. 10th AIAA/ASME Joint Thermophysics and Heat Transfer Conference, 28 June ~ 1 July, 2010, Chicago, Illinois. AIAA-2010-5053 (2010)
- 3. Nawaz, A., Loehle, S., Herdrich, G., Martinez, E.: Comparison of Calorimetric Sensors NASA Ames and IRS. 44th AIAA Thermophysics Conference, San Diego, CA. AIAA-2013-3018 (2013)
- 4. Loehle, S., Nawaz, A., Herdrich, G., Fasoulas, S., Martinez, E., Raiche, G.: Comparison of Heat Flux Gages for High Enthalpy Flows - NASA Ames and IRS. 46th AIAA Thermophysics Conference, Washington, D.C. AIAA-2016-4422 (2016)
- 5. Birch, B., Buttsworth, D., Loehle, S., Hufgard, F.: Fast-Response transient heat flux measurements in a plasma wind tunnel. International Journal of Heat and Mass Transfer 173. (2021)
- 6. Hermann, T., Loehle, S., Zander, F., Fasoulas, S.: Measurement of the aerothermodynamic state in a high enthalpy plasma wind-tunnel flow. Journal of Quantitative Spectroscopy & Radiative Transfer. Vol. 201, 216-225 (2017)
- 7. Gardon, R.: An Instrument for the Direct Measurement of Intense Thermal Radiation, Review of Scientific Instruments. Vol. 24, No. 5 (1953)
- 8. Guelhan, A., Esser, B., Vecchio, A.D., Loehle, S., Sauvage, N., Chazot, O., Asma, C.O.: Comparative Heat Flux Measurements on Standard Models in Plasma Facilities. AIAA/CIRA 13th International Space Planes and Hypersonics Systems and Technologies. AIAA-2005-3324 (2005)
- 9. Loehle, S., Fasoulas, S., Herdrich, G., Hermann, T., Massuti-Ballester, B., Meindl, A., Pagan, A.S., Zander, F.: The Plasma Wind Tunnels at the Institute of Space Systems: Current Status and Challenges. 32nd AIAA Aerodynamic Measurement Technology and Ground Testing Conference, Washington, D.C. AIAA-2016-3201 (2016)
- 10. Loehle, S., Nawaz, A., Herdrich, G., Fasoulas, S., Martinez, E., Raiche, G.: Comparison of Heat Flux Gages for High Enthalpy Flows - NASA Ames and IRS. 46th AIAA Thermophysics Conference, Washington, D.C. AIAA-2016-4422 (2016)
- 11. Loehle, S., Hermann, T., Zander, F.: Experimental assessment of the performance of ablative heat shield materials from plasma wind tunnel testing. CEAS Space Journal. Vol. 10, pp. 203-211 (2018)
- 12. Pope, R.B.: Stagnation-Point Convective Heat Transfer in Frozen Boundary Layers. AIAA Journal, Vol. 6, No. 4 (1968)
- 13. Zoby, E.V., Sullivan, E.M.: Effects of Corner Radius on stagnation-Point Velocity Gradients on Blunt Axisymmetric Bodies. Journal of Spacecraft. Vol. 3, No. 10
- 14. Stoeckle, T.: Investigation of the surface calalytic properties of metallic and ceramic materials in high enthalpy flows. Institute of Space Systems University of Stuttgart. (2000)
- 15. Nawaz, A., Driver, D., Terrazas-Salinas, I.: Surface Catalysis and Oxidation on Stagnation Point Heat Flux Measurements in High Enthalpy Arc Jets. Fluid Dynamics and Co-located Conference, San Diego, CA. AIAA-2013-3138 (2013)
- 16. Marschall, J., Copeland, R.A., Hwang, H.H., Wright, M.J.: Surface Catalysis Experiments on Metal Surfaces in Oxygen and Carbon Monoxide Mixtures. 44th AIAA Aerospace Sciences Meeting and Exhibit, Reno, Nevada. AIAA-2013-3138 (2013)
- 17. Gökçen, T., Balboni, J.A., Alunni, A.I.: Computational Simulations of the 10-MW TP3 Arc-Jet Facility Flow. 45th AIAA Thermophysics Conference, Dallas, TX. AIAA-2015-3103 (2015)

HiSST-2025-0005 Page | 17 Investigation of Heat flux and Stagnation Pressure Integrated Measurement Probe using Gardon Gauge